Supplement of Atmos. Meas. Tech., 16, 1147–1165, 2023
https://doi.org/10.5194/amt-16-1147-2023-supplement

Atmospheric Measurement Techniques
Open Access
EGU

Supplement of

Characterization of offline analysis of particulate matter with FIGAERO-CIMS

Jing Cai et al.

Correspondence to: Kaspar R. Daellenbach (kaspar.daellenbach@psi.ch) and Claudia Mohr (claudia.mohr@psi.ch)

Supplementary information

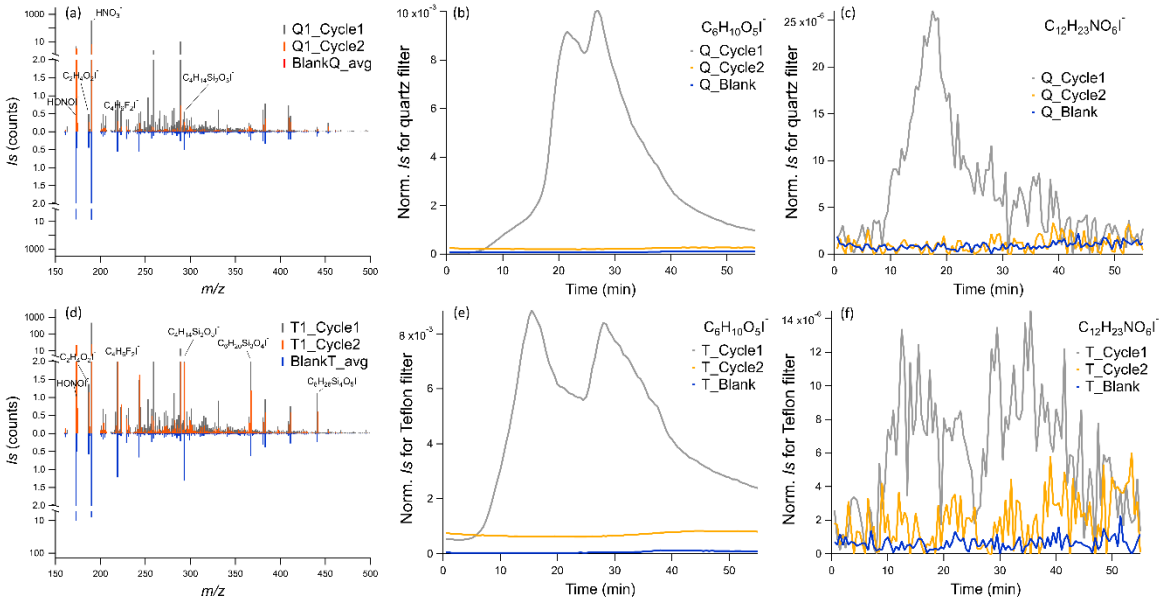

Figure S1. Comparison of the integrated raw signals from heating, reheating cycles and ambient blanks for (a) Quartz fiber filters and (d) Teflon filters, thermograms of $C_6H_{10}O_5I^-$ (b) and $C_{12}H_{23}NO_6I^-$ (c) of heating and reheating cycles for Quartz fiber filters, and thermograms of $C_6H_{10}O_5I^-$ (e) and $C_{12}H_{23}NO_6I^-$ (f) of heating and reheating cycles for Teflon filters.

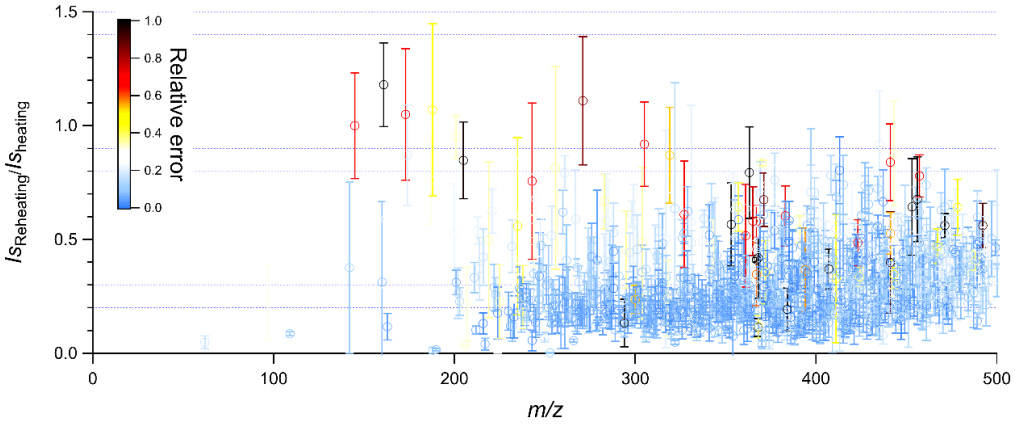

Figure S2. The average *Is* ratios between reheating and heating cycles for the Quartz filter with the standard deviations for the three reheating tests. Dots were colored by the relative errors (defined as the Std/Avg of *Is* from the duplicate tests) of compounds

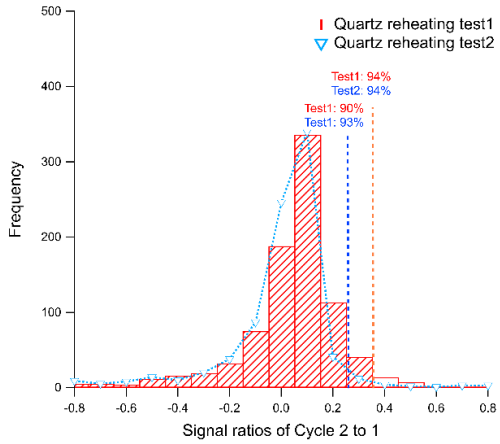

Figure S3. The distribution of *Is* ratios from reheating/heating for 0.75 and 1.2 μg loading Quartz samples. The negative value is caused by the low signals of the reheating cycles and background subtractions.

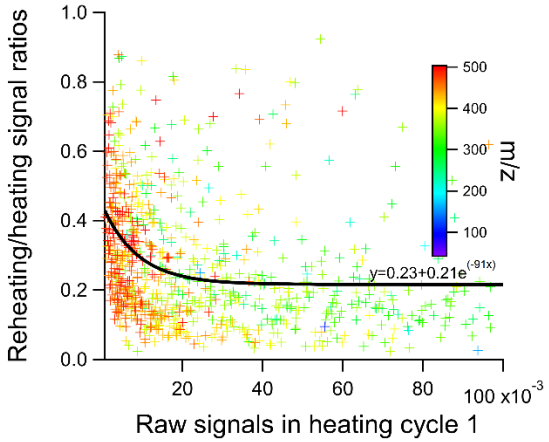

Figure S4. Exponential fit for reheating/heating signal ratios

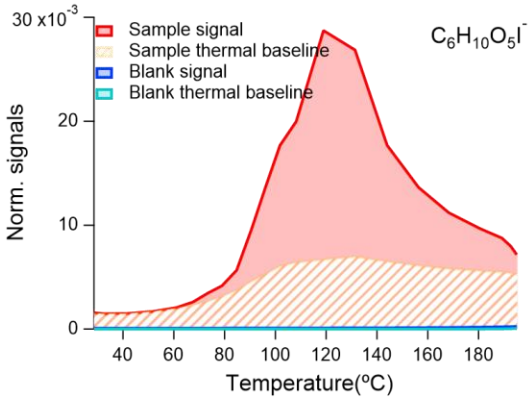

Figure S5. Thermograms for $C_6H_{10}O_5I^-$ of sample and field blank (blk), and the thermal baselines for sample and blanks using background subtraction Method 4

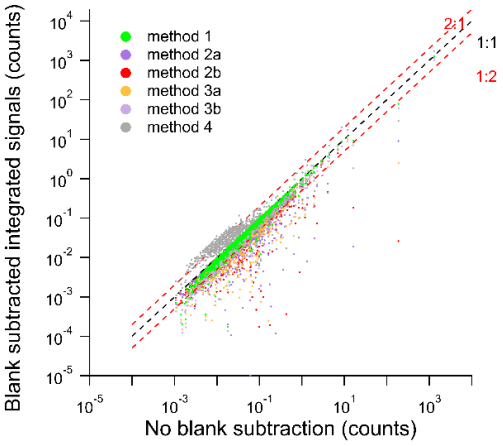

Figure S6. Comparison of the integrated signals for the 24-h samples for different blank subtraction methods

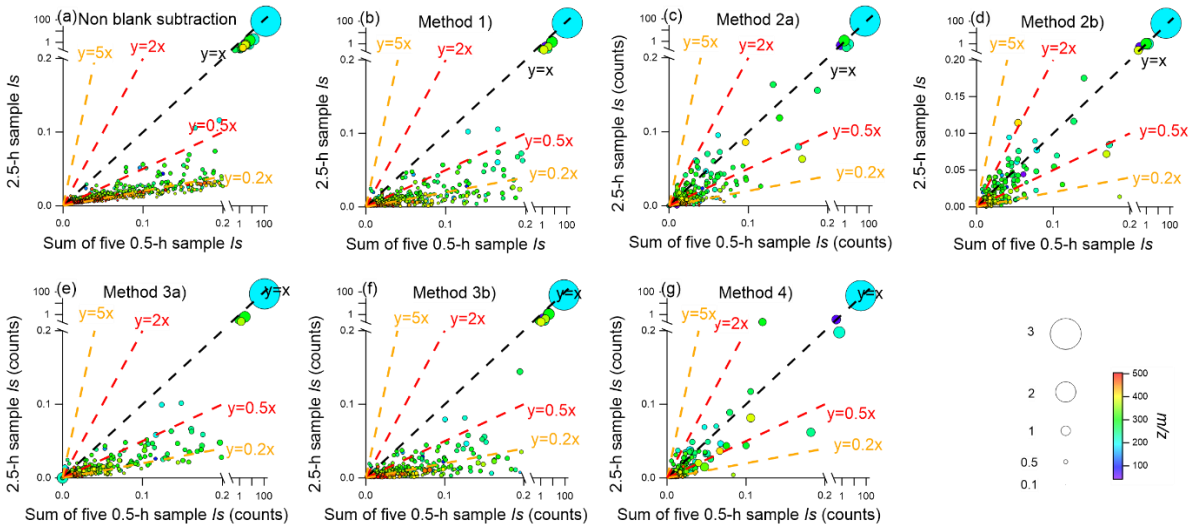

Figure S7. Comparison of the integrated signals (*Is*) of all compounds for the 2.5-h versus the sum of signals of five 0.5-h samples (a) without blank subtraction, with blank subtraction using (b) Method 1, (c) Method 2a, (d) Method 2b, (e) Method 3a, (f) Method 3b, (g) Method 4. The size of dots is proportional to the 4th root of integrated signal intensities of compounds, and they are color-coded by the ions' m/z (mass-to-charge ratio). Compounds with *Is*<0.2 are shown on a linear scale and compounds with *Is*>0.2 on a log scale

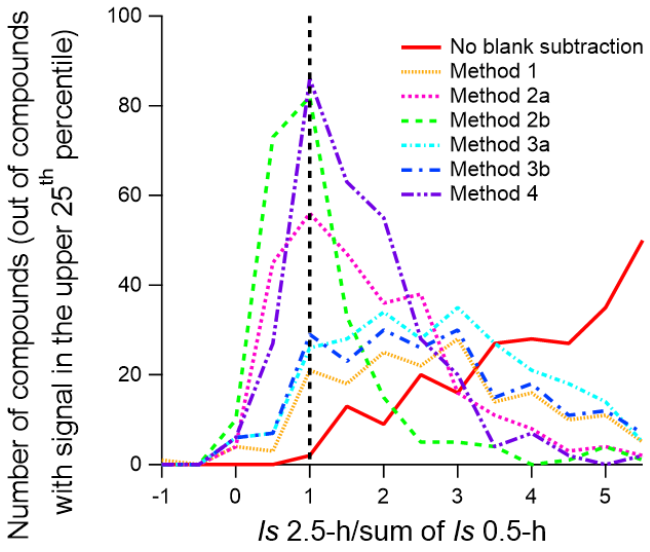

Figure S8. The distribution of *Is* ratios between the 2.5-h and the sum of five 0.5-h samples for the 25% of compounds with the highest signal intensity for different background subtraction methods. The distribution range is from -1 to 6 with bins of 0.5, which covers 82%, 61%, 94%, 93%, 90%, 72%, and 96% of the top 25% of compounds with respect to signal for no blank subtraction, Method 1, 2a, 2b, 3a, 3b, and 4, respectively.

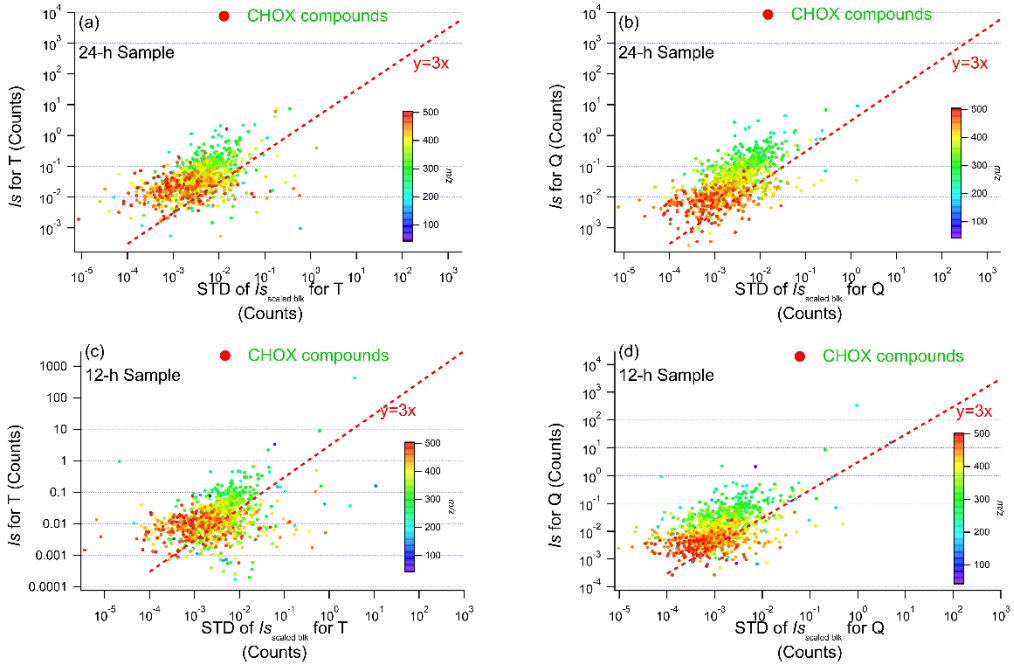

Figure S9. Comparison of the raw CHOX integrated signal intensities (*Is*) and standard deviations of the corresponding backgrounds (scaled field blanks) for (a) 24-h Teflon, (b) 12-h Quartz, (c) 12-h Teflon, and (d) 12-h Quartz samples

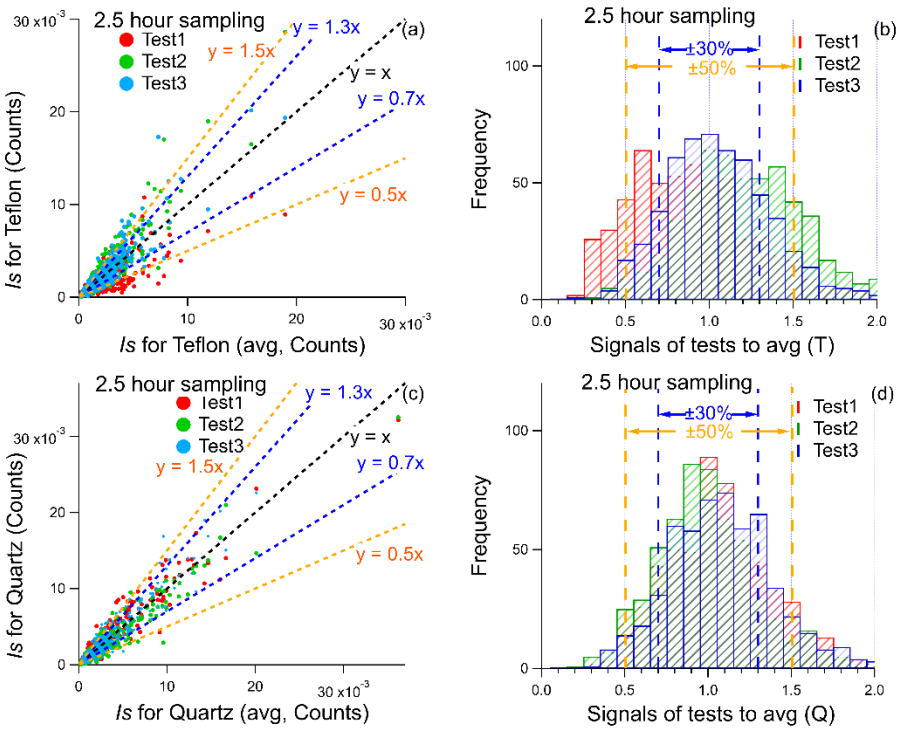

Figure S10. Comparison of the integrated signal intensities for the 3 duplicate tests of the 2.5-h sample for the (a) Teflon and (c) quartz fiber filters, the histogram of the distributions of the ratios of the 3 duplicate tests to their average for (b) Teflon and (d) Quartz fiber filters

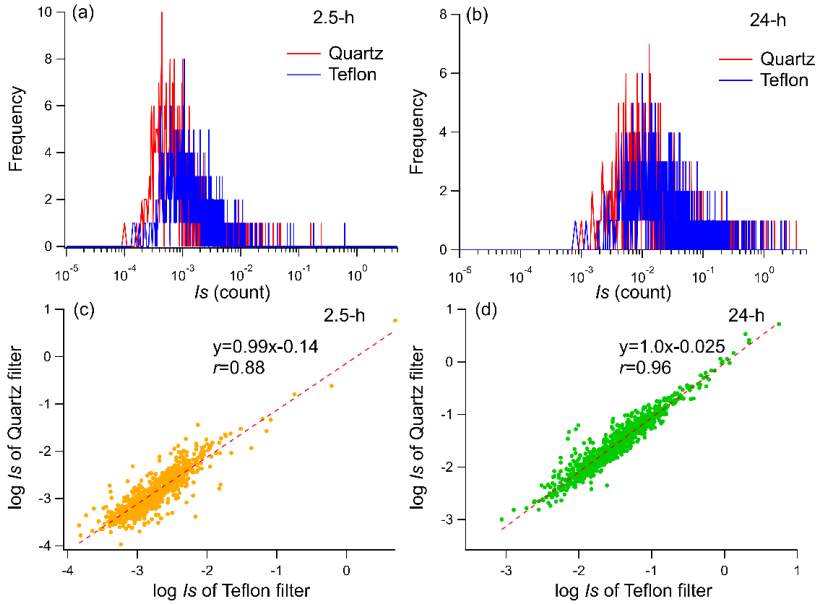

Figure S11. Frequency distribution of the integrated signals of CHOX compounds for Quartz and Teflon samples in (a) 2.5-h collection time (bin width: 1×10^{-5} counts), (b) 24-h collection time (bin width: 1×10^{-4} counts). The correlations between log-transformed *Is* of Quartz and Teflon samples from (c) 2.5-h, and (d) 24-h samples.

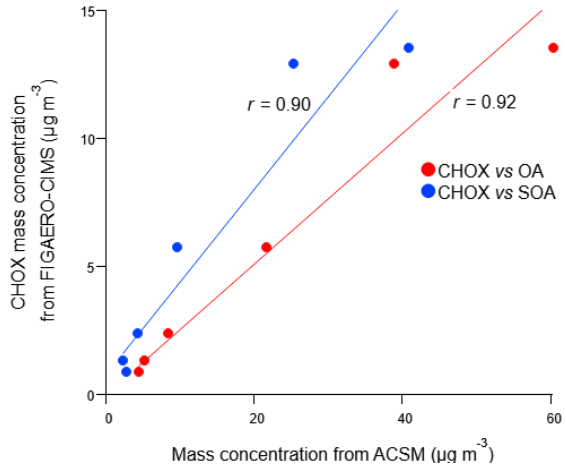

Figure S12. Comparison between CHOX mass concentrations from FIGAERO-CIMS, organic aerosols (OA), and secondary organic aerosols (SOA) derived from ToF-ACSM at the Peking University Campus (PKU) site. Calibrations for FIGAERO-CIMS were conducted for a series of chemical compounds with both the permeation tube and micro-syringes. The details of the site, comparison setting up, calibrations, and calculations can be found in Zheng et al. (2021).

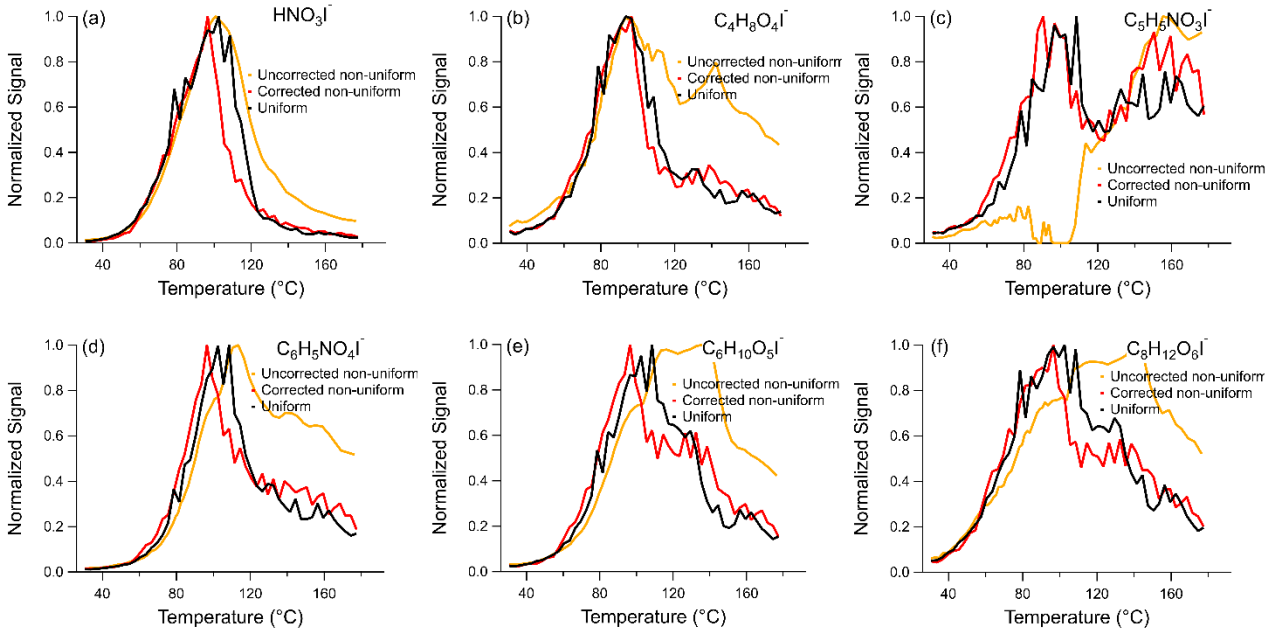

Figure S13. Thermograms (normalized to the highest signal) from the 24h Teflon sample with/without correction from non-uniform ramping and uniform ramping protocols, (a) HNO_3I^-, (b) $C_4H_8O_4I^-$, (c) $C_5H_5NO_3I^-$, (d) $C_6H_5NO_4I^-$, (e) $C_6H_{10}O_5I^-$, (f) $C_8H_{12}O_6I^-$

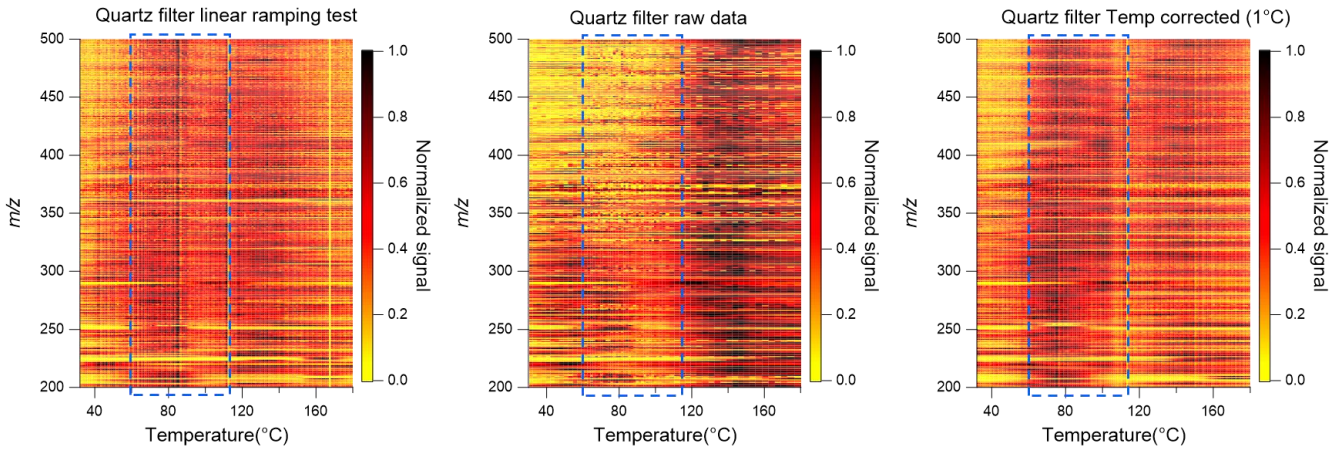

Figure S14. Two-dimensional (2D) thermograms of CHOX compounds for the Quartz filter in (a) the fast linear ramping, (b) the intermediate ramping without correction, and (c) the intermediate ramping after correction. The blue dashed box marks the slow temperature rate region.

Table S1 Sampling information and mass loadings on the punches for the thermogram comparison of different filter types (T is for Teflon; Q is for quartz fiber)

Sampling date	Sampling time	Filter type	$PM_{2.5}$ loading (μg/2mm punch, 0.031 cm^2)	OA loading (μg/punch)
6-Nov	21:30–9:00	T and Q	0.57	0.38
8-Nov	21:30–9:00	T and Q	1.49	0.61
13-Nov	9:30–21:00	T and Q	4.84	1.01
	21:30–9:00	T and Q	5.57	1.15
24-Nov	9:30–9:00	T and Q (3 duplicate tests)	3.03	1.25

Reference

Zheng, Y., Chen, Q., Cheng, X., Mohr, C., Cai, J., Huang, W., Shrivastava, M., Ye, P., Fu, P., Shi, X., Ge, Y., Liao, K., Miao, R., Qiu, X., Koenig, T. K., and Chen, S.: Precursors and Pathways Leading to Enhanced Secondary Organic Aerosol Formation during Severe Haze Episodes, Environ Sci Technol, 55, 15680-15693, 10.1021/acs.est.1c04255, 2021.